PHYSICAL REVIEW D VOLUME 14, NUMBER 12 15 DECEMBER 1976

Multiple direct exchange in a Yang-Mills theory at high energy*

Barry M. McCoy†
Institute for Theoretical Physics, State University of New York, Stony Brook, New York 11794

Tai Tsun Wu
Gordon McKay Laboratory, Harvard University, Cambridge, Massachusetts 02138
(Received 10 February 1976)

For eighth and higher orders, we obtain the leading high-energy behavior of the sum of all one-layer Feynman diagrams in Yang-Mills theory. These are the contributions from Feynman diagrams where the two incident fast particles exchange directly Yang-Mills bosons that are much less energetic. The incident particles may be either bosons or fermions of arbitrary isospin, and the result is also generalized to include the case of the Higgs scalar. The scattering amplitudes in all these cases are closely related, and all behave as $s\ln^{n-1}s$ in the $2n+2$ order. Furthermore, in this leading order for $n \geq 2$, the exchanged isospins are always 0 and 2, no matter how high the isospins of the incident particles are.

I. INTRODUCTION

We continue[1] in this paper the study of the high-energy behavior of two-body scattering amplitudes in the Yang-Mills theory with a Higgs mechanism by calculating the behavior in $(2n+2)$-order perturbation theory (for $n \geqslant 3$) of the sum of all diagrams which involve the multiple direct exchange of $n+1$ Yang-Mills bosons between the two energetic particles. We will consider the cases (see Fig. 1) where the incident particles are either fermions of arbitrary isospin, spin-one bosons of isospin 1, spin-zero bosons of arbitrary isospin, or a Higgs scalar.

This study is a part of our continuing investigation[2,3] of the behavior of quantum field theories at high energy by perturbation-theory methods. Most of this program has involved the extracting, in each order of perturbation theory, of the leading behavior (in terms of powers of $\ln s$) of the scattering amplitude as $s\to\infty$. This is, of course, only a first step in the understanding of high-energy behavior, since, as seen explicitly in the case of elastic scattering in massive quantum electrodynamics,[3] the sum of these leading logarithms can be expected to violate unitarity (and in particular the Froissart bound). To obtain the physical behavior of the scattering amplitude suitable nonleading logarithms must be included. Some indication of the role of these nonleading logarithms may be seen in a recent study of the 2-point function of the 2-dimensional Ising model where *all* the logarithms were computed and summed.[4] However, before these effects can be studied, the leading terms must be understood and therefore in this paper we will study the multiple direct-exchange diagrams (for Yang-Mills theory) which, in massive quantum electrodynamics,[5] proved to be so useful in obtaining the physical predictions of the rising cross section.[6]

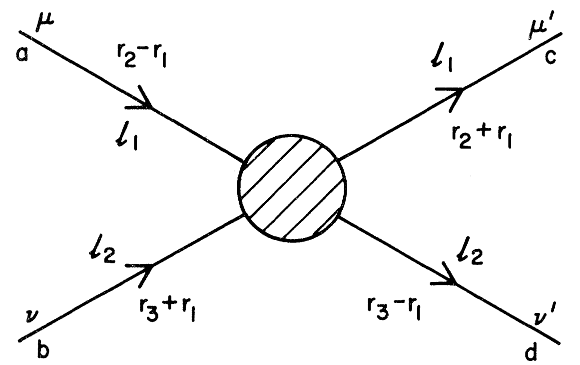

FIG. 1. The kinematics for the scattering of a particle of isospin l_1 from a particle of isospin l_2. The particles may be either bosons or fermions.

Several of these multiple direct-exchange diagrams are shown in Fig. 2. When at least one of the fast incident particles is a fermion or a spin-zero boson, the leading $s\to\infty$ behavior comes from the region of momentum space where the two fast momenta go through the diagram as shown in Fig. 3. When both of the incident particles are spin-one bosons, this region of momentum space will still contribute to the leading $s\to\infty$ behavior but there may be other paths for the fast momenta which also contribute (Fig. 4). In this paper we will not investigate these other possible momentum regions and by the term "multiple direct-exchange diagram" we will always mean that the fast momenta are restricted to flow, as shown in Fig. 4(a).

Our results are summarized as follows. In $(2n+2)$-order perturbation theory where $n+1$ bosons are exchanged, the sum of all multiple direct-exchange graphs in leading order as $s\to\infty$ where the incident particles are spin-zero bosons of isospin l_1 and l_2 is

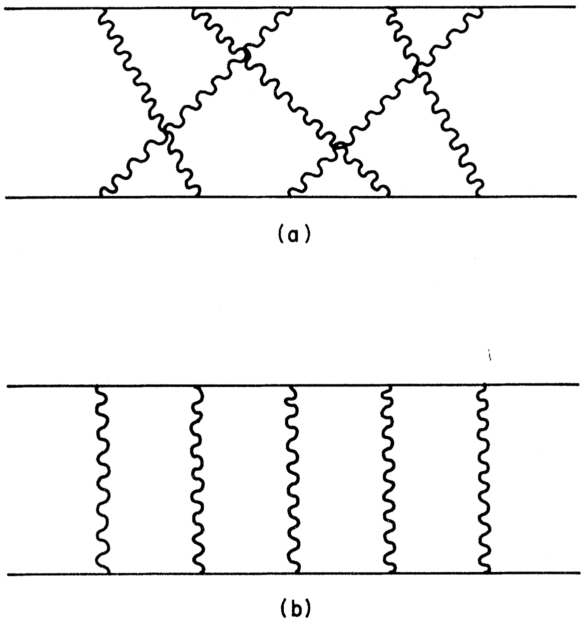

FIG. 2. Two tenth-order multiple-direct-exchange Feynman diagrams for the scattering of two fermions. It will be shown that diagram (a) contributes to leading order as $s\to\infty$ whereas diagram (b) does not.

$$\mathfrak{M}^{D(n)}_{S(l_1),S(l_2)} \sim 4g^{2n+2}\pi i s\,\frac{1}{(n-1)!}\ln^{n-1}s\,K_{n+1}(t)\times\left[\tfrac{1}{3}2^{n-3}\vec{\sigma}^{(1)2}\vec{\sigma}^{(2)2}T^{(0)}+(-1)^{n+1}2T^{(2)}\right], \tag{1.1}$$

where

$$T^{(0)}=1^{(1)}1^{(2)}, \tag{1.2a}$$

$$T^{(2)}=\tfrac{1}{2}\left(\{\sigma^{(1)}_m,\sigma^{(1)}_n\}-\tfrac{2}{3}\vec{\sigma}^{(1)2}\delta_{mn}1^{(1)}\right)\times\left(\{\sigma^{(2)}_m,\sigma^{(2)}_n\}-\tfrac{2}{3}\vec{\sigma}^{(2)2}\delta_{mn}1^{(2)}\right) \tag{1.2b}$$

($\{A,B\}=AB+BA$). The isospin matrices satisfy

$$[\sigma_a,\sigma_b]=-\epsilon_{abc}\sigma_c,\quad a\neq b \tag{1.3a}$$

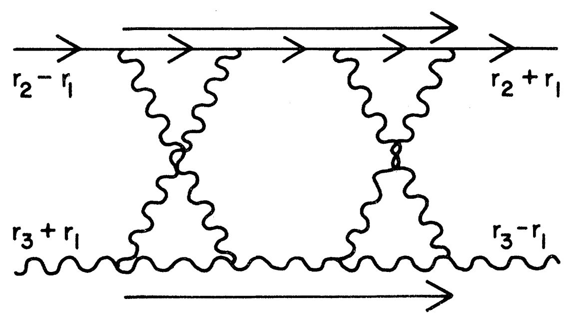

FIG. 3. An eighth-order multiple-direct-exchange Feynman diagram for fermion-boson scattering indicating the path which the large momentum r_2 and r_3 must take.

and

$$\vec{\sigma}^2=-l(l+1), \tag{1.3b}$$

and

$$K_{n+1}(t)=\int\frac{d^2k_1}{(2\pi)^3}\cdots\frac{d^2k_n}{(2\pi)^3}(\vec{k}_1^{\,2}+\lambda^2)^{-1}\cdots(\vec{k}_n^{\,2}+\lambda^2)^{-1}\times[(\vec{k}_1+\vec{k}_2+\cdots+\vec{k}_n-\vec{\Delta})^2+\lambda^2]^{-1}. \tag{1.4}$$

We note explicitly that

$$T^{(2)}=0\ \text{ if } l_1=\tfrac{1}{2}\ \text{ or }\ l_2=\tfrac{1}{2} \tag{1.5a}$$

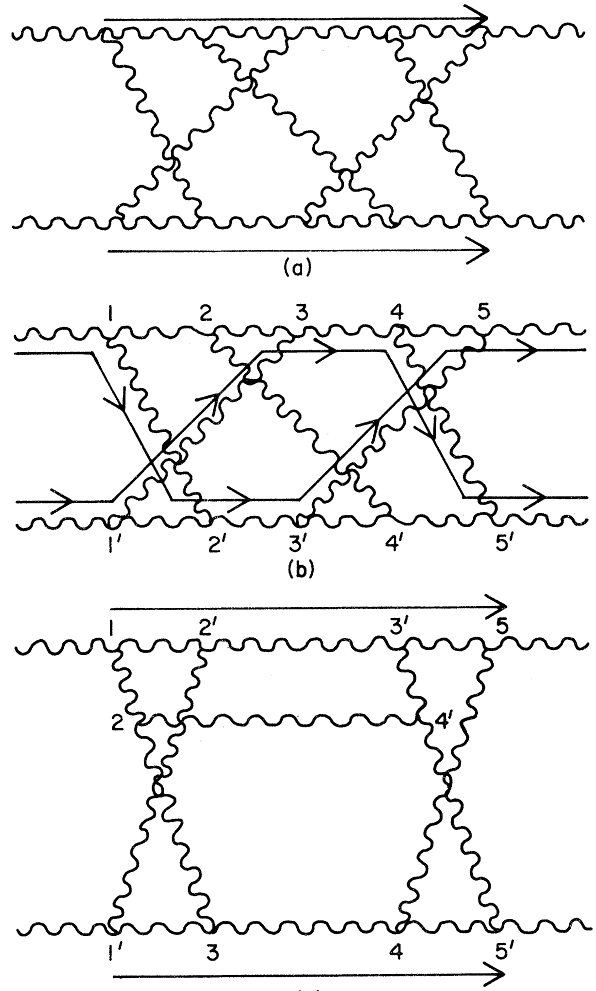

FIG. 4. (a) A tenth-order boson-boson Feynman diagram with the path of fast momenta which are considered for multiple direct exchange indicated. (b) A second path for the large-r_2 and large-r_3, momenta which is not considered for multiple direct exchange. The r_2 momenta are to flow in the path 12′3′5 and the r_3 momenta are to flow in the path 1′345′. (c) A redrawing of the previous diagram where the path 12′3′5 is at the top and the path 1′345′ is at the bottom. This momenta path is *not* included in multiple-direct exchange.

and that if $l_1 = l_2 = 1$

$$T^{(2)}_{ab,cd} = \delta_{ab}\,\delta_{cd} + \delta_{ad}\,\delta_{bc} - \tfrac{2}{3}\delta_{ac}\,\delta_{bd}\,. \tag{1.5b}$$

From this basic amplitude we find

$$\mathfrak{M}^{D(n)}_{BB} \sim \mathfrak{M}^{D(n)}_{S(1)S(1)}\,\delta_{1,1'}\,\delta_{2,2'}\,, \tag{1.6a}$$

$$\mathfrak{M}^{D(n)}_{BF(l)} \sim (2m)^{-1}\mathfrak{M}^{D(n)}_{S(1)S(l)}\,\delta_{1,1'}\,\delta_{2,2'}, \tag{1.6b}$$

$$\mathfrak{M}^{D(n)}_{F(l_1)F(l_2)} \sim (2m)^{-2}\mathfrak{M}^{D(n)}_{S(l_1)S(l_2)}\delta_{1,1'}\delta_{2,2'}\,, \tag{1.6c}$$

$$\mathfrak{M}^{D(n)}_{BS(l)} \sim \mathfrak{M}^{D(n)}_{S(1)S(l)}\,\delta_{1,1'}\,, \tag{1.6d}$$

and

$$\mathfrak{M}^{D(n)}_{F(l_1)S(l_2)} \sim (2m)^{-1}\mathfrak{M}^{D(n)}_{S(l_1)S(l_2)}\,\delta_{1,1'}\,. \tag{1.6e}$$

Furthermore, we find that amplitudes involving Higgs scalars are obtained from the amplitude in which the Higgs scalar is replaced by an isospin-$\frac{1}{2}$ spin-zero boson. Thus we explicitly have

$$\mathfrak{M}^{D(n)}_{HS(l)} \sim 4g^{2n+1}\pi i s\,\frac{1}{(n-1)!}\,\ln^{n-1}s \times K_{n+1}(t)2^{n-5}l(l+1)\delta_{ac} \tag{1.6f}$$

(where a and c are the isospin indices of the scalar boson),

$$\mathfrak{M}^{D(n)}_{HH} \sim 4g^{2n+1}\,\pi i s\,\frac{1}{(n-1)!}\,\ln^{n-1}s\;K_{n+1}(t)(3)\,2^{n-7}, \tag{1.6g}$$

$$\mathfrak{M}^{D(n)}_{HB} \sim \mathfrak{M}^{D(n)}_{HS(1)}\,\delta_{2,2'}\,, \tag{1.6h}$$

and

$$\mathfrak{M}^{D(n)}_{HF(l)} \sim (2m)^{-1}\mathfrak{M}^{D(n)}_{HS(l)}\,\delta_{2,2'}\,. \tag{1.6i}$$

In (1.6) $\delta_{j,j'}$ is 1 if the spin of particle j is not flipped and zero if the spin is flipped (and the spin of the vector bosons may be either transverse or longitudinal).

We obtain these results by an application of the momentum-space techniques previously introduced.[2,3] However, in an attempt to keep this paper reasonably self-contained we will summarize these techniques in Sec. II.

In Sec. III we will analyze the high-energy behavior of the relevant Feynman diagrams. In Sec. IV we will combine the results of these expansions with the isospin factors to obtain the result (1.1).

II. FORMULATION OF THE PROBLEM

In this section we will derive in detail the relation of the amplitudes $\mathfrak{M}_{BB}, \mathfrak{M}_{BF(l)}, \mathfrak{M}_{F(l_1)F(l_2)}$ to the amplitude $\mathfrak{M}_{S(l_1)S(l_2)}$ and we will summarize the techniques of momentum-flow diagrams in a form suitable for the present problem.

A. Isospin matrices

When the fast particle is a fermion of isospin $\frac{1}{2}$ the interaction with the Yang-Mills field is

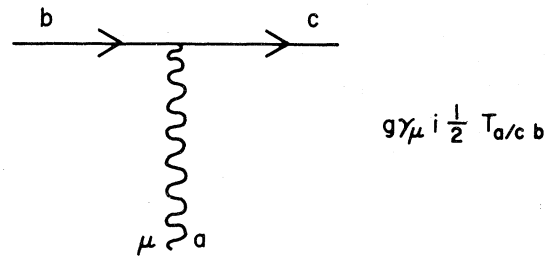

FIG. 5. The fermion-boson vertex.

given by the vertex of Fig. 5, where τ_a are the Pauli matrices. Note that the row indices correspond to the final fermion and the column index corresponds to the initial fermion. For the interaction of a fermion of isospin l with the Yang-Mills boson we merely replace

$$i\tfrac{1}{2}\tau_a \rightarrow \sigma_a\,,$$

where the $(2l+1)$-dimensional matrices σ_a satisfy (1.3).

When the fast particle is a boson of isospin 1

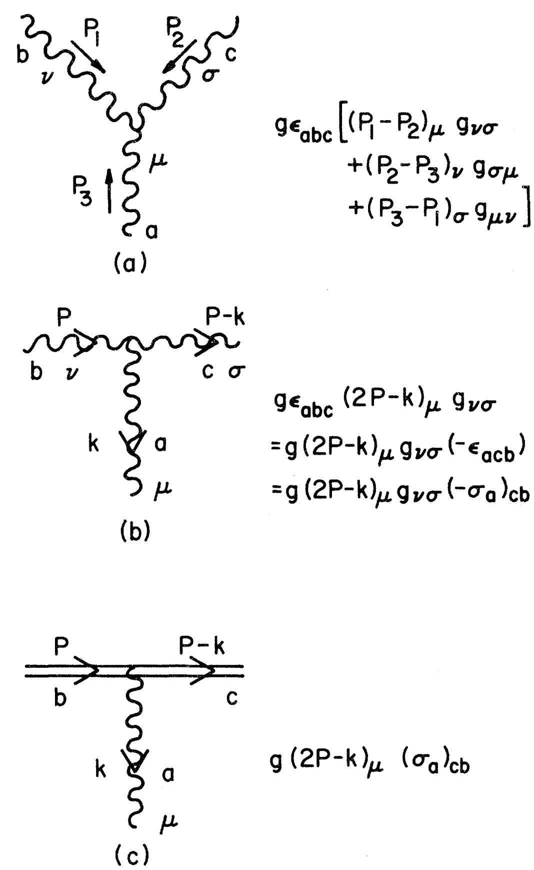

FIG. 6. (a) The three-boson vertex when all 3 bosons have isospin 1. (b) The only term in the three-boson vertex that need be considered for the calculation of the leading $s\rightarrow\infty$ behavior when a fast momentum P flows through two of the boson lines.

the interaction with the Yang-Mills boson is given in Fig. 6(a). However, from this, if we specialize to the path where p_1 and p_2 carry the fast momentum P, then of the 3 terms in Fig. 6(a) only the one term of Fig. 6(b) contributes to leading order. Then, to write the isospin factor ϵ_{abc} in a matrix form with the convention used for fermions that the outgoing fast particle is represented by the row index of σ_a and the incoming fast particle is represented by the column index of σ_a, see that

$$g\epsilon_{abc}(2P-k)_\mu g_{\nu\sigma}=g(2P-k)_\mu g_{\nu\sigma}(-\epsilon_{acb})$$
$$=g(2P-k)_\mu g_{\nu\sigma}(-\sigma_a)_{cb}\,, \qquad (2.1)$$

where with $l=1$

$$\sigma_a\big|_{cc'}=\epsilon_{acc'}\,. \qquad (2.2)$$

B. Reduction of numerators

Using the results of the previous subsection we find that at high energy the amplitude in $(2n+2)$-order perturbation theory for one of the $(n+1)!$ multiple-direct-exchange diagrams is

$$\begin{aligned}\mathfrak{M}^{D(n)}_{j_1,j_2}(P)\sim(-i)^{n+2}g^{2n+2}\int\frac{d^4k_1}{(2\pi)^4}\cdots\frac{d^4k_n}{(2\pi)^4}&N^{j_1}_{\mu_1,\ldots,\mu_{n+1};a_1,\ldots,a_{n+1}}(r_2,r_1,k_1,\ldots,k_n)\\&\times N^{j_2}_{\mu_{P_1},\ldots,\mu_{P_{n+1}};a_{P_1},\ldots,a_{P_{n+1}}}(r_3,-r_1,-k_{P_1},\ldots,k_{P_n})\\&\times(k_1^2-\lambda^2)^{-1}(k_2^2-\lambda^2)^{-1}\cdots(k_n^2-\lambda^2)^{-1}[(k_1+\cdots+k_n-2r_1)^2-\lambda^2]^{-1}\\&\times[(r_2-r_1-k_1)^2-m^2]^{-1}[(r_2-r_1-k_1-k_2)^2-m^2]^{-1}\cdots\\&\times[(r_2-r_1-k_1-\cdots-k_n)^2-m^2]^{-1}\\&\times[(r_3+r_1+k_{P_1})^2-m^2]^{-1}[(r_3+r_1+k_{P_1}+k_{P_2})^2-m^2]^{-1}\cdots\\&\times[(r_3+r_1+k_{P_1}+\cdots+k_{P_n})^2-m^2]^{-1},\end{aligned} \qquad (2.3)$$

where P is a permutation of $1,2,\ldots,n+1$ and j_1 and j_2 are either B, F, or S with [Fig. 7(a)]

$$\begin{aligned}N^{F(l)}_{\mu_1,\mu_2,\ldots,\mu_{n+1};a_1,a_2,\ldots,a_{n+1}}(r,r_1,k_1,\ldots,k_n)=(i)^n\bar u(r+r_1)\gamma_{\mu_{n+1}}\sigma_{a_{n+1}}(\not r-\not r_1-\not k_1-\cdots-\not k_n+m)\\\times\gamma_{\mu_n}\sigma_{a_n}(\not r-\not r_1-\not k_1-\cdots-\not k_{n-1}+m)\cdots\gamma_{\mu_2}\sigma_{a_2}(\not r-\not r_1-\not k_1+m)\\\times\gamma_{\mu_1}\sigma_{a_1}u(r-r_1)\end{aligned} \qquad (2.4a)$$

and [Fig. 7(b)]

$$\begin{aligned}N^{B}_{\mu_1,\ldots,\mu_{n+1};a_1,\ldots,a_{n+1}}(r,r_1,k_1,\ldots,k_n)=(-i)^n\epsilon'_{\mu'}g_{\mu'\nu_{2n}}(2r-k_1-\cdots-k_n)_{\mu_{n+1}}(-\sigma_{a_{n+1}})g_{\nu_{2n}\nu_{2n-1}}\\\times g_{\nu_{2n-1}\nu_{2n-2}}(2r-2r_1-2k_1-\cdots-2k_{n-1}-k_n)_{\mu_n}(-\sigma_{a_n})g_{\nu_{2n-2}\nu_{2n-3}}\\\times\cdots g_{\nu_2\nu_1}(2r-2r_1-k_1)_{\mu_1}(-\sigma_{a_1})g_{\nu_1\mu}\epsilon_\mu,\end{aligned} \qquad (2.4b)$$

where ϵ_μ and ϵ'_μ are the polarization vectors of the incoming and outgoing bosons, and [Fig. 7(c)]

$$\begin{aligned}N^{S(l)}_{\mu_1,\ldots,\mu_{n+1};a_1,\ldots,a_{n+1}}(r,r_1,k_1,\ldots,k_n)=(i)^n(2r-k_1-\cdots-k_n)_{\mu_{n+1}}(\sigma_{a_{n+1}})\\\times(2r-2r_1-2k_1-\cdots-2k_{n-1}-k_{n-1}-k_n)_{\mu_n}(\sigma_{a_n})\cdots\\\times(2r-2r_1-k_1)_{\mu_1}(\sigma_{a_1}).\end{aligned} \qquad (2.4c)$$

Since we are considering the momentum region where all k_n are small compared to r_2 or r_3 we may simplify (2.4) by dropping $r_1,k_1,\ldots,k_n$ in comparison to r. Then in (2.4a) we anticommute $\not r$ to the right and may drop all terms where $\not r$ acts on $\bar u(r+r_1)$ by means of the Dirac equation. Therefore we find

$$\begin{aligned}N^{F(l)}_{\mu_1,\ldots,\mu_{n+1};a_1,\ldots,a_{n+1}}&\sim(i)^n(2r)_{\mu_2}\cdots(2r)_{\mu_{n+1}}\sigma_{a_{n+1}}\sigma_{a_n}\cdots\sigma_{a_1}\bar u(r+r_1)\gamma_{\mu_1}u(r-r_1)\\&\sim(i)^n(2m)^{-1}(2r)_{\mu_1}\cdots(2r)_{\mu_{n+1}}\sigma_{a_{n+1}}\sigma_{a_n}\cdots\sigma_{a_1}\delta_{l,l'},\end{aligned} \qquad (2.5a)$$

$$\begin{aligned}N^{B}_{\mu_1,\ldots,\mu_{n+1};a_1,\ldots,a_{n+1}}&\sim-(i)^n(2r)_{\mu_1}\cdots(2r)_{\mu_{n+1}}\sigma_{a_{n+1}}\cdots\sigma_{a_1}\epsilon'_{\mu'}g_{\mu'\nu_{2n}}g_{\nu_{2n}\nu_{2n-1}}g_{\nu_{2n-1}\nu_{2n-2}}\cdots g_{\nu_1\mu}\epsilon_\mu\\&=-(i)^n(2r)_{\mu_1}\cdots(2r)_{\mu_{n+1}}\sigma_{a_{n+1}}\cdots\sigma_{a_1}\epsilon'_{\mu'}g_{\mu'\mu}\epsilon_\mu,\end{aligned} \qquad (2.5b)$$

and

$$N^{S(l)}_{\mu_1,\ldots,\mu_{n+1};a_1,\ldots,a_{n+1}}\sim(i)^n(2r)_{\mu_1}\cdots(2r)_{\mu_{n+1}}\sigma_{a_{n+1}}\cdots\sigma_{a_1}. \qquad (2.5c)$$

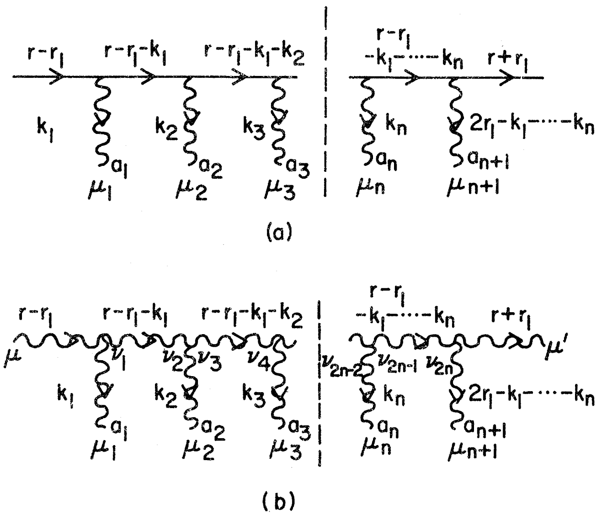

FIG. 7. (a) A fermion line carrying the large momentum r and the $n+1$ exchanged bosons attached to it. (b) A boson line carrying the large momentum r and the $n+1$ exchanged bosons attached to it.

To reduce (2.5b) further consider first the case of boson-fermion scattering with $r=r_2$. In the frame where the incoming momentum $p_1=r_2-r_1$ is $((\lambda^2+\omega^2)^{1/2}, \omega, 0, 0)$ the two transverse polarization vectors are

$$\epsilon^{(1)}=(0,0,1,0), \quad \epsilon^{(2)}=(0,0,0,1) \tag{2.6a}$$

and the longitudinal polarization vector is

$$\epsilon^{(L)}=\frac{1}{\lambda}(\omega, (\lambda^2+\omega^2)^{1/2}, 0, 0). \tag{2.6b}$$

All 3 of these polarization vectors satisfy $p_1\cdot\epsilon=0$ and $\epsilon^2=-1$. We may use the consequence of gauge invariance that

$$\epsilon_{\mu'}\mathfrak{M}_{\mu'\mu}p_{1\mu}=0\ , \tag{2.7}$$

where $\mathfrak{M}_{\mu',\mu}$ is the complete gauge-invariant amplitude to replace $\epsilon^{(L)}$ by

$$\begin{aligned}\bar\epsilon^{(L)}&=\epsilon^L-\frac{1}{\lambda}p_1\\ &=\frac{1}{\lambda}[\omega-(\omega^2+\lambda^2)^{1/2}](1,1,0,0).\end{aligned} \tag{2.8}$$

As $\omega\to\infty$

$$\bar\epsilon^{(L)}\sim-\frac{\lambda}{2\omega}(1,-1,0,0). \tag{2.9}$$

We may now take the Lorentz transform of the polarization vector (2.6) and (2.9) back to the frame where

$$\begin{aligned}p_1&=r_2-r_1\\ &=((\omega^2+\lambda^2+r_\perp^{\,2})^{1/2}, \omega, r_\perp, 0)\end{aligned} \tag{2.10}$$

to find approximately for $\omega\to\infty$

$$\begin{aligned}\epsilon^{(1)}&\sim\left(-\frac{r_\perp^{\,3}}{\omega^2\lambda}, -\left(1+\frac{r_\perp^{\,4}}{2\omega^2\lambda^2}\right)\frac{r_\perp}{\omega}, 1-\frac{r_\perp^{\,2}}{2\omega^2}, 0\right)\\ &\sim(0,0,1,0),\end{aligned} \tag{2.11a}$$

$$\epsilon^{(2)}=(0,0,0,1), \tag{2.11b}$$

$$\begin{aligned}\bar\epsilon^{(L)}&\sim-\frac{\lambda}{2\omega}\left(1-\frac{r_\perp^{\,2}}{\omega\lambda}, -1+\frac{r_\perp^{\,2}}{\omega\lambda}, -\frac{r_\perp}{\omega}, 0\right)\\ &\sim-\frac{\lambda}{2\omega^2}r_3\ .\end{aligned} \tag{2.11c}$$

For the polarization vector of the outgoing boson we have

$$\begin{aligned}\epsilon'^{(1)}&\sim(0,0,1,0),\\ \epsilon'^{(2)}&\sim(0,0,0,1),\\ \epsilon'^{(L)}&\sim\frac{1}{\lambda}\left(\omega+\frac{r_\perp^{\,2}}{\lambda}+\frac{r_\perp^{\,4}}{2\omega\lambda^2}, \omega+\frac{r_\perp^{\,2}}{\lambda}\right.\\ &\qquad\left.+\frac{1}{2\omega}\left(\lambda^2-r_\perp^{\,2}+\frac{r_\perp^{\,4}}{\lambda^2}\right), -r_\perp, 0\right)\\ &\sim\frac{1}{\lambda}r_2.\end{aligned} \tag{2.12}$$

Therefore in (2.4b)

$$\epsilon'^{(1)}_{\mu'}g_{\mu',\mu}\epsilon^{(1)}_{\mu}\sim-1, \tag{2.13a}$$

$$\epsilon'^{(2)}_{\mu'}g_{\mu',\mu}\epsilon^{(2)}_{\mu}\sim-1, \tag{2.13b}$$

$$\epsilon'^{(L)}_{\mu'}g_{\mu',\mu}\bar\epsilon^{(L)}_{\mu}\sim-\frac{1}{2\omega^2}r_2\cdot r_3\sim-1 \tag{2.14}$$

and so for boson-fermion scattering we may use

$$N^B_{\mu_1,\ldots,\mu_{n+1};a_1,\ldots,a_{n+1}}(r_2)\sim(i)^n(2r)_{\mu_1}\cdots(2r)_{\mu_{n+1}}\sigma_{a_{n+1}}\cdots\sigma_{a_1}\delta_{1,1'}, \tag{2.15}$$

where $\delta_{1,1'}$ is 1 if the polarizations of the incoming and outgoing bosons are the same and zero otherwise.

For the case of boson-boson scattering we may use (2.7) on one of the incoming boson indices. Moreover, while the analog of (2.7) with both incoming polarization vectors replaced by the corresponding momenta is not ture, it still holds approximately as $\omega\to\infty$ and hence (2.15) may be used for all cases. Therefore we have the reduction

$$N^B\sim N^{S(1)}\delta_{1,1'}, \tag{2.16a}$$

$$N^{F(l)}\sim(2m)^{-1}N^{S(l)}\delta_{1,1'}. \tag{2.16b}$$

Thus it suffices to consider the scattering of two scalar bosons of isospin l_1 and l_2 where

$$N^{S(l)}_{\mu_1,\ldots,\mu_{n+1};a_1,\ldots,a_{n+1}} N^{S(l_2)}_{\mu_{P_1},\ldots,\mu_{P_{n+1}};a_{P_1},\ldots,a_{P_{n+1}}} = (-1)^n (4r_2 \cdot r_3)^{n+1} \sigma^{(1)}_{a_{n+1}} \sigma^{(1)}_{a_n} \cdots \sigma^{(1)}_{a_1} \sigma^{(2)}_{a_{P_{n+1}}} \sigma^{(2)}_{a_{P_n}} \cdots \sigma^{(2)}_{a_{P_1}}. \tag{2.17}$$

C. Momentum-flow diagrams

The reduced numerator (2.17) no longer depends on the integration variables and therefore the momentum-space techniques discussed in detail in the previous study of sixth- and tenth-order perturbation theory of massive quantum electrodynamics[2,3] may be directly applied. We will here summarize and specialize the discussion of those papers in a form adapted to the present problem. For a more complete discussion we refer the reader to Refs. 2 and 3.

The essence of the technique is to use, instead of the momentum components k_0 and k_3, the components

$$k_\pm = k_0 \pm k_3, \tag{2.18a}$$

with

$$dk_0 dk_3 = \tfrac{1}{2} dk_+ dk_-, \tag{2.18b}$$

to use the approximation that as $\omega \to \infty$

$$r_{2+} \sim 2\omega, \quad r_{2-} \sim 0, \tag{2.19a}$$

$$r_{3+} \sim 0, \quad r_{3-} \sim 2\omega, \tag{2.19b}$$

and

$$r_{1\pm} \sim 0, \tag{2.19c}$$

and then to do all integrations over plus components of momenta by contour integration. The result of this integration depends in what region of minus momentum space the variables $k_{-1}, \ldots, k_{-n}$ lie.

As shown in Ref. 2 we may determine the various allowed regions of k_{-j} space by drawing sets of arrows on the lines of the Feynman diagram. The arrows represent the direction of flow of the minus component of momentum in the lines and are drawn according to the following rules:

(1) At least one arrow must point towards and one arrow away from each vertex that does not connect to an external line.

(2) If an external line carries no minus momentum as $\omega \to \infty$ (such as $r_2 \pm r_1$), then on the two internal lines that connect to it one arrow must point towards the vertex and the other arrow must point away from the vertex.

(3) The incoming line that carries the momentum r_3 acts as a source of minus momentum (the arrows on the two internal lines connecting to it point away from the vertex).

(4) The outgoing line that carries the momentum r_3 acts as a sink of minus momentum (the arrows on the two internal lines connecting to it point towards the vertex).

(5) There are no closed loops in which all arrows point in the same direction around the loop.

Each configuration of arrows will be considered individually as a separate momentum-flow diagram and for each separate momentum-flow diagram we will in general choose a different set of integration variables $q_{\pm j}$ (which are linear combinations of $k_{\pm l}$). In general, the poles closed upon in the process of evaluating the integrals over plus components of momenta will be different depending on which momentum-flow diagram is considered. For a given momentum-flow diagram the poles are determined by the following:

(1) First one must choose some momentum loop.

(2) In this loop there will be arrows pointing in both directions. All propagators with an arrow in one of the two directions (clockwise or counterclockwise) must be closed upon. We indicate the pole used by a cross on the line.

(3) For each pole chosen in this manner a second momentum loop not containing this pole is chosen and the process of closing on poles is repeated. This process is carried out until all n plus momenta have been integrated.

This process of determining poles to close on is very nonunique. However, for the multiple-direct-exchange diagrams there is a particular choice of poles that is very useful. This choice of poles is determined because we have the additional restriction that we are considering only regions of momentum space where all $k_{\pm j}$ are small compared with 2ω. This leads to two important restrictions on the allowed momentum-flow diagrams:

(1) The arrows on the bottom line must all point from left to right.

(2) No crosses may be put on the upper line.

With these two restrictions we consider the bottom line of a typical multiple-direct-exchange diagram along with $n+1$ vertical lines attached to it (Fig. 8). The arrows on the vertical lines are separated into two classes:

(1) a set on the left which points up, and

(2) a set on the right which points down.

There can be no more classes because the transition from down on the left to up on the right would [by restriction (1)] lead to a configuration such as Fig. 8(b) which, since all 3 arrows shown point in the same direction and since the loop is completed by arrows in the upper horizontal line which by restriction (2) cannot be closed upon, will give zero when the integration of the

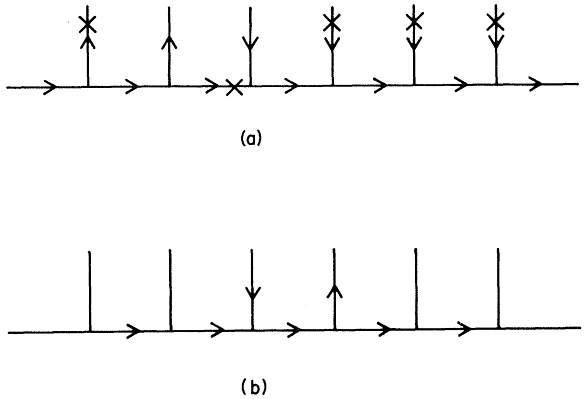

FIG. 8. (a) The bottom half of an allowed one-layer momentum-flow diagram illustrating the choice of poles closed on. (b) The bottom half of a one-layer momentum-flow diagram which illustrates why the configuration of a down arrow on the left and an up arrow on the right will not contribute.

plus momentum around this loop is carried out. Accordingly, once the arrows are drawn there is only one set of contributing poles which is specified as follows:

(1) the one propagator on the bottom line which separates the up arrows from the down arrows; and

(2) the $n-1$ propagators for the vertical lines which do not intersect with the propagator chosen in step (1).

We now carry out the integration over the plus components of momenta. This leads to an integrand (of the minus and $\perp$ integrals) which contains the following factors:

(1) for each propagator of momentum p_l closed upon the factor

$$-2\pi i|p_{l-}|^{-1} \tag{2.20a}$$

and the rest of the factors evaluated with

$$p_{l+}=p_{l-}^{-1}(\vec{p}_{\perp l}{}^2+\lambda^2); \tag{2.20b}$$

(2) for the lower lines without the cross

$$(2\omega p_{l+}-\vec{p}_{\perp l}{}^2-m^2+i\epsilon)^{-1}\sim(2\omega)^{-1}p_{l+}{}^{-1}; \tag{2.21}$$

(3) for the upper lines

$$\frac{1}{\pm 2\omega p_{l-}-\vec{p}_{\perp l}{}^2-m^2+i\epsilon}\sim\frac{1}{2\omega}\,\frac{1}{\pm p_{l-}-O(1/\omega)+i\epsilon}, \tag{2.22}$$

where the p_{l-} are always chosen positive and the sign $\pm$ is chosen to be plus if the arrows point from left to right (positive p_{l+}) and to be minus if the arrow points from right to left (negative p_{l+});

(4) for the two vertical lines with no crosses

$$(p_{l+}p_{l-}-\vec{p}_{\perp l}{}^2-\lambda^2+i\epsilon)^{-1}. \tag{2.23}$$

We thus find that $\mathfrak{M}^{D(n)}_{S(l_1)S(l_2)}$ of (2.3) is given as

$$\mathfrak{M}^{D(n)}_{S(l_1)S(l_2)}(P)\sim-2s\,g^{2n+2}\sigma^{(1)}_{a_{n+1}}\cdots\sigma^{(1)}_{a_1}\sigma^{(2)}_{a_{P_{n+1}}}\cdots\sigma_{a_{P_1}}\sum\int\frac{d^2k_1}{(2\pi)^3}\cdots\frac{d^2k_n}{(2\pi)^3}\int dq_1\cdots dq_n\,\mathcal{G}(q_1,\ldots,q_n), \tag{2.24}$$

where

(1) the sum is over all momentum-flow diagrams satisfying restrictions (1) and (2),

(2) the minus momentum coordinates q_i are chosen to satisfy

$$0\le q_i\le 2\omega, \tag{2.25}$$

and

(3) the integrand $\mathcal{G}(q_1,\ldots,q_n)$ is constructed with the factors

(a) $p_{l-}{}^{-1}$ for each cross on a vertical line with momentum p_l,

(b) $p_{l+}{}^{-1}$ for each bottom horizontal line of momentum p_l with no cross,

(c) $(p_{l+}p_{l-}-\vec{p}_l{}^2-\lambda^2+i\epsilon)$ for each of the two vertical lines with no cross,

(d) $[\pm p_{l-}-O(1/\omega)+i\epsilon]^{-1}$ for each horizontal line on top where the + (−) sign is used if the arrow is from left to right (right to left).

The maximum power of $\ln s$ which can come from any integral of the form $\int dq_1\cdots dq_n\mathcal{G}(q_1,\ldots,q_n)$ is $\ln^n s$. This leading behavior comes from a region of the q_i space

$$0<q_{Q_1}\ll q_{Q_2}\ll\cdots\ll q_{Q_n}\ll 2\omega \tag{2.26}$$

such that

$$\mathcal{G}(q_1,\ldots,q_n)\sim\frac{1}{q_1}\,\frac{1}{q_2}\cdots\frac{1}{q_n}. \tag{2.27}$$

For each ordering (2.26) for which (2.27) holds, the integral under the summation sign of (2.24) reduces to

$$(m_1,m_2)K_{n+1}(t), \tag{2.28}$$

where $K_{n+1}(t)$ is given by (1.4) and

$$(m_1,m_2)=\frac{1}{n!}\,[m_1\ln^n s+m_2(\ln^n s-n\pi i\ln^{n-1}s)], \tag{2.29}$$

with $m_1=0$ and $m_2=\pm 1$ or $m_2=0$ and $m_1=\pm 1$.

The calculation of (2.24) thus reduces to

(1) determination of the allowed momentum-flow diagrams,

(2) determination of the allowed momentum

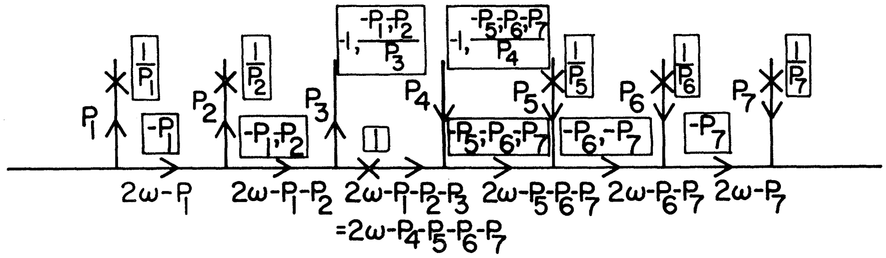

FIG. 9. The lower line and the vertical lines attached to it. The particular case illustrated is for $n=6$. The poles closed on are indicated by crosses and the factors associated with each line are given in the box next to the line. Where two or more factors appear in the box the smallest factor is to be chosen.

orderings, and
(3) determination of the pair (m_1, m_2).

III. CALCULATION OF THE MOMENTUM-FLOW DIAGRAMS

We present the calculation of the momentum-flow diagrams in the following 7 subsections.

A. Ordering of momenta on the lower line

Consider the lower line and the vertical lines attached to it as shown in Fig. 9. The factors associated with each line are shown in a box next to the line and when two or more factors are in the same box the smallest factor must be chosen. The $n+1$ momenta p_i satisfy

$$\sum \text{upward } p\text{'s} = \sum \text{downward } p\text{'s}. \qquad (3.1)$$

There are n factors of the form $1/\sum a_i q_i$ (with $q_i = 0,\ 1,$ or -1) which come from the n propagators on the upper line. It is then seen from Fig. 9 that the only way for there to be an ordering of momenta such that the integrand of the q integration is

$$\prod_{i=1}^{n} \frac{1}{q_i} \qquad (3.2)$$

is for the momenta on the left of the cross on the lower line to be ordered

$$p_1 \gg p_2 \gg p_3 \gg \cdots \qquad (3.3a)$$

and for the momenta on the right of the cross on the lower line to be ordered

$$p_{n+1} \gg p_n \gg p_{n-1} \gg \cdots\ . \qquad (3.3b)$$

When this ordering occurs, the factors of p_i from the bottom lines cancel the factors of $1/p_i$ from the $n-1$ crosses on the vertical lines and the -1 must be used on each of the two uncrossed vertical lines. Therefore, with restriction (3.3) the factor which the lower part of the momentum-flow diagram contributes to the integrand is

$$(-1)^{n+1}. \qquad (3.4)$$

B. The necessity of a bridge

Consider the leftmost and rightmost vertical lines which connect to the lower line. Because this leftmost vertical line carries the largest upward momenta and this rightmost vertical line carries the largest downward momenta and because of (3.1), the largest elementary momentum q_n must flow in these outermost vertical lines (and in no others). Moreover, since we must have only one factor of $1/q_n$ from the upper line, this q_n may flow in only *one* upper line segment. Therefore these two outermost vertical lines can be connected to the top line in only the two ways shown in Fig. 10. Either of these two structures

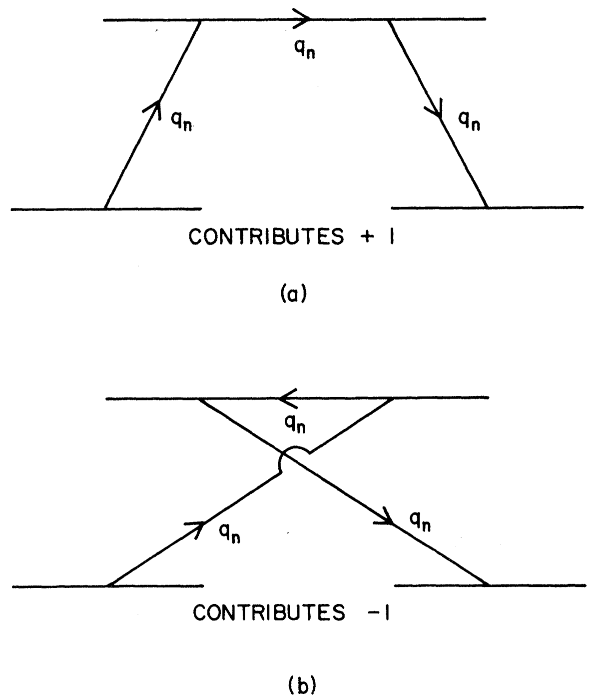

FIG. 10. The two possible paths which q_n, the largest elementary momentum, may follow. Both of these structures will be called a bridge.

will be called a bridge. If the only difference between two Feynman diagrams is the difference between the two possible bridges of Fig. 10, then to leading order in $\ln s$ these two Feynman diagrams will cancel because the bridge of Fig. 10(a) contributes the factor of $+1$ while the bridge of Fig. 10(b) contributes the factor of -1 (and all the other factors in the two diagrams will be the same).

C. Ordered momentum-flow diagrams

There are now $n-1$ elementary momenta left to be chosen and $n-1$ propagators left in the upper line. We will expand our notion of a momentum-flow diagram to that of an ordered momentum-flow diagram by making the definition that

$$q_1 \ll q_2 \ll \cdots \ll q_{n-1} \ll q_n . \tag{3.5}$$

Each distinct way that coordinates q_l satisfying (3.5) can be put on a momentum-flow diagram will be called an ordered momentum-flow diagram. In order to obtain (3.2) the momenta q_l can be the maximum momenta in one and only one of the upper propagators. We can thus discuss all possible contributions to a given momentum-flow diagram by assigning momenta $q_1, \ldots, q_{n-1}$ and the associated arrows to the upper $n-1$ line segments consistent with (3.5) and with the arrows on the vertical lines of the diagram. This will give for each ordered momentum-flow diagram the contribution of

$$(-1)^{\text{number of left-pointing upper arrows}} \times \begin{cases} (0,1) \text{ if } q_1 \text{ points right,} \\ (1,0) \text{ if } q_1 \text{ points left.} \end{cases} \tag{3.6}$$

D. Combination of ordered momentum-flow diagrams

Our next step is to demonstrate that not all ways in which the momentum-flow diagrams may be closed on the top by arrows with momenta $q_1, \ldots, q_{n-1}$ need be considered when all ordered momentum-flow diagrams contributing to a given Feynman diagram are summed.

When arrows are drawn on the top line they may either connect a vertical line in a connected fashion to the original bridge formed by q_n or at some stage a second bridge may be formed. An example of these two choices is shown in Fig. 11.

Consider first the situation shown in Fig. 11(b) where after some state there is a second bridge which is separated from the segments connected to the q_n bridge by one line. On this free link we may draw the arrow with momentum q in *either* direction and still satisfy all necessary requirements without changing anything else in

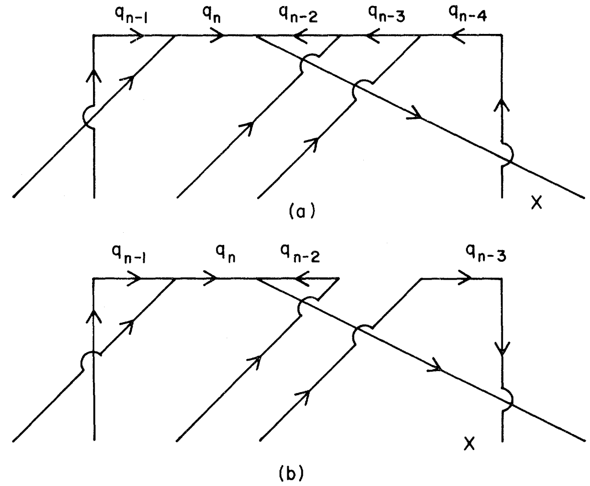

FIG. 11. (a) An example of part of an ordered momentum-flow diagram where all the momenta in the upper line are connected inwards to the q_n bridge. (b) An example of an ordered momentum-flow diagram where the momentum q_{n-3} forms a second bridge.

the diagram. But if q_m is not q_1 (the smallest momentum) the only difference between the contributions from these two ordered momentum-flow diagrams is the sign which comes from the reversal of the q_m arrow. Therefore these two related ordered momentum-flow diagrams cancel. The only exception to this cancellation is if q_m is the smallest momenta since $(0,1)$ and $(-1,0)$ clearly do not cancel.

Similarly ordered momentum-flow diagrams with 3 or more bridges, each separated from each other by one free link, must always cancel in the sum because only one of the two (or more) free momenta can be smallest. Furthermore, the contribution from ordered momentum-flow diagrams which at some stage have a second bridge separated from the main bridge by more than one free link will also cancel out in the sum, as the example of Fig. 12 illustrates. Therefore we are left with only those ordered momentum-flow diagrams such that

(1) at no stage is there more than one bridge, or

(2) if there are two bridges at some stage, then the second bridge must be separated from the rest of diagram by precisely one link which must carry the smallest momentum q_1.

Thus far we have only combined ordered momentum-flow diagrams with the cross on the lower horizontal line in the same place. To effect further cancellations we must combine diagrams with crosses in different places. Consider the situation shown in Fig. 13 where there is a second bridge which is separated from the main bridge by the smallest momenta and there is an extra line which carries the next-to-smallest momenta. Because the smallest momenta is on the free link between the two bridges this next-to-smallest momenta must be *next to the lower cross*. But this cross may be on either side of this next-smallest momentum line and for a given direction of q_1 on the free link the contribution from these two related ordered momentum-flow diagrams differ only by the sign coming from the direction of the q_2 arrow. Therefore they cancel in the sum and hence if there is a second bridge it must carry the second-smallest momenta q_2.

E. Construction of the contributing diagrams

From the preceding discussion we see that with the exception of the two smallest momenta q_1 and q_2 is suffices to specify which vertical line the momenta q_l flows in because on the top of the diagram the momenta is forced to flow in that link which joins the vertical line carrying q_l with that part of the diagram which involves $q_{l+1}, \ldots, q_n$. Therefore at any stage in the construction of an ordered momentum-flow diagram we have at most 4 choices for the vertical line which q_l may flow in. The momenta q_n must flow in a bridge. Then relative to the momenta which are connected to this bridge the new vertical line carrying momenta q_l may have its lower end either at the right or at the left inside of the bridge and its upper end at the right or left outside of the bridge. We symbolically represent these four possibilities by $\frac{i}{j}$, where $i=R$ or L specifies where the top of the vertical line is added and $j=R$ or L specifies where the bottom of the vertical line is added. Then from Fig. 14 we see that these four possibilities give the following factors to the product (3.6):

$$\frac{R}{R}\Rightarrow 1, \quad \frac{L}{L}\Rightarrow 1, \quad \frac{R}{L}\Rightarrow -1, \quad \frac{L}{R}\Rightarrow -1. \qquad (3.7)$$

F. The two smallest momenta

To complete our study of ordered momenta-flow diagrams we must determine the possible ways in which the last two vertical lines may be added to the diagram. By definition these last two lines will be next to each other on the bottom. However, on the top there are two possibilities: (1) Either the two lines are on different sides of the

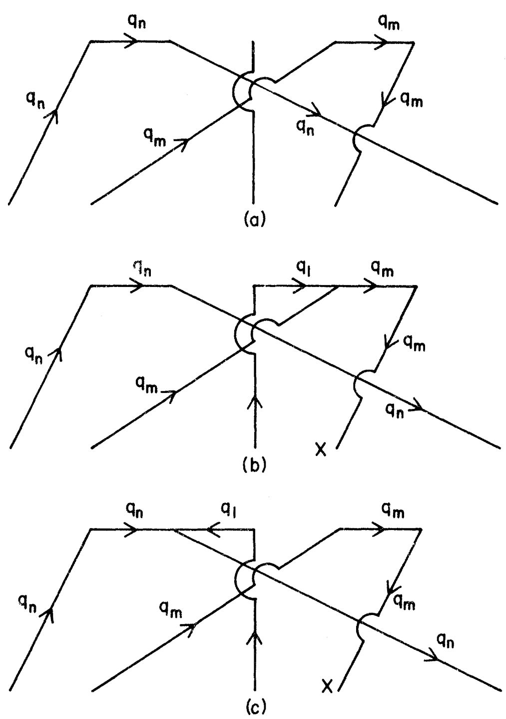

FIG. 12. (a) An example of an ordered momentum-flow diagram where at some stage (denoted here by q_m) a second bridge is separated from the main bridge (shown here simply as the main q_n bridge) by two (or more) links. (b) and (c) illustrate the two different ways in which a momentum q_l (which is not smallest) may be drawn in the diagram (a). The arrows on the remaining upper link may point in either direction. All the diagrams from (b) cancel the corresponding diagrams coming from (c).

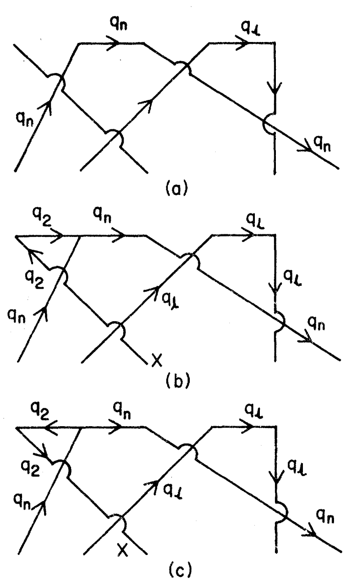

FIG. 13. (a) An example of part of an ordered momentum-flow diagram with a second bridge (denoted here by q_l) separated from the main connected bridge (denoted here simply by q_n) by a free link with momentum q_1. (b) and (c) are the demonstration of the cancellation of the pair of ordered momentum-flow diagrams derived from (a) which differ only in the location of the cross (or equivalently by the direction of q_2).

bridge or (2) they are on the same side of the bridge. The second possibility is examined in Fig. 15 and then we see that there are 4 contributing ordered momentum-flow diagrams, two of which have the smallest momentum q_1 between two bridges, where q_2 flows in one bridge, and two of which never have a two-bridge structure at any stage. It is explicitly seen from Fig. 15 that these four ordered momentum-flow diagrams cancel out. Therefore the last-two-smallest momenta must flow in vertical lines which *cannot be added to the same side on top*.

It thus remains to compute the contribution coming from the four remaining possibilities of $\substack{RL\\RL}$, $\substack{LR\\LR}$, $\substack{LR\\RL}$, $\substack{RL\\LR}$ (where the smallest momentum is on the left). This calculation is displayed in Fig. 16, where we find

$$\substack{RL\\RL} \Rightarrow (-1,1), \quad \substack{LR\\LR} \Rightarrow (-1,1),$$
$$\substack{LR\\RL} \Rightarrow (1,-1), \quad \substack{RL\\LR} \Rightarrow (1,-1). \tag{3.8}$$

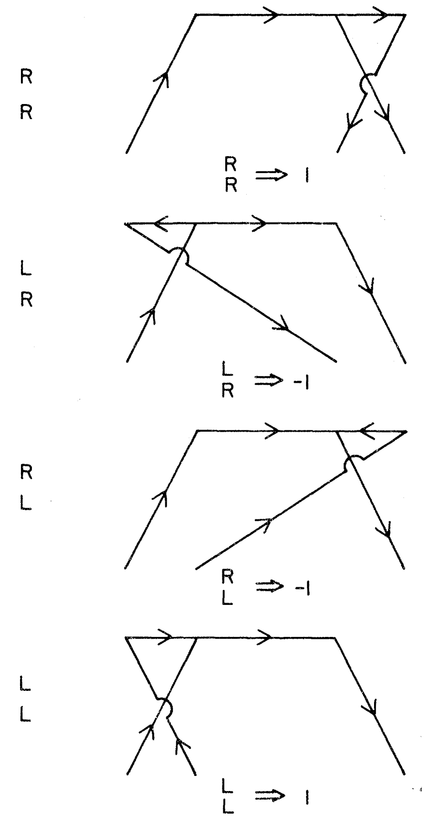

FIG. 14. The four possible ways a vertical line may be added to the lines connected to the q_n bridge and the factor which each configuration gives to the contribution of the ordered momentum-flow diagram.

G. Examples of calculations

We use the results of Eqs. (3.4), (3.7), and (3.8) to evaluate several examples.

(a) In eighth order ($n=3$) consider the Feynman diagram of Fig. 17. The only possible momentum orderings for this diagram are

$$\substack{RL\\RL} + \substack{LR\\RR}$$

so from (3.4) and (3.8) the diagram has the contribution $2(-1,1)$.

(b) In tenth order ($n=4$) consider the two diagrams of Fig. 18. The first diagram has the two possible momentum orderings

$$\left(\substack{RL\\RL} + \substack{LR\\LR}\right)\substack{R\\R} \Rightarrow -2(-1,1) \tag{3.9}$$

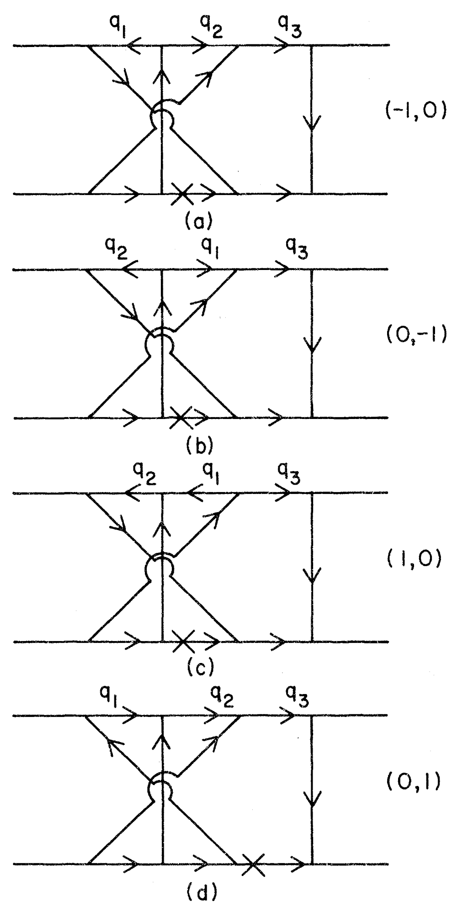

FIG. 15. The demonstration of the cancellation of the four (classes of) ordered momentum-flow diagrams which occurs when the last two vertical lines considered lie on the same side of the bridge on top. The diagram explicitly shown is an eighth-order diagram but the q_3 bridge may be replaced by a connected bridge with any number of momenta and the same argument goes through.

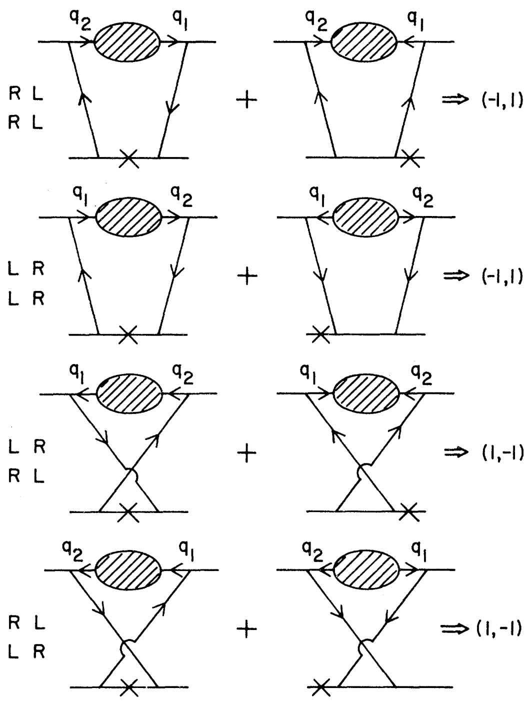

FIG. 16. The calculation of the contribution to the ordered momentum-flow diagram from the four possible ways of adding the two smallest momenta q_1 and q_2.

and the second has the orderings

$$\left(\genfrac{}{}{0pt}{}{RL}{RL}+\genfrac{}{}{0pt}{}{LR}{LR}\right)\genfrac{}{}{0pt}{}{R}{L}=2(-1,1). \tag{3.10}$$

(c) In the twelfth order ($n=5$) we consider as an example the diagram of Fig. 19. Here there are 4 possible momentum orderings,

$$\left(\genfrac{}{}{0pt}{}{RL}{RL}+\genfrac{}{}{0pt}{}{LR}{LR}\right)\left(\genfrac{}{}{0pt}{}{RL}{RL}+\genfrac{}{}{0pt}{}{LR}{LR}\right)=4(-1,1). \tag{3.11}$$

IV. SUMMATION OF FEYNMAN DIAGRAMS

If we were interested in the separate contributions of each Feynman diagram which contributes to multiple-direct exchange in $(2n+2)$-order perturbation theory we would be faced with the problem of determining the possible orderings of the factors $\genfrac{}{}{0pt}{}{R}{R}, \genfrac{}{}{0pt}{}{L}{R}, \genfrac{}{}{0pt}{}{R}{L}, \genfrac{}{}{0pt}{}{L}{L}$ for each diagram and we would have to work out the corresponding isospin factors. However, we are *not* interested in the separate contribution of individual Feynman diagrams but are only interested in their sum. Therefore further simplification is possible because at *each* stage of building up a contributing Feynman diagram we may use either $\genfrac{}{}{0pt}{}{R}{R}$, $\genfrac{}{}{0pt}{}{L}{L}$, $\genfrac{}{}{0pt}{}{R}{L}$, or $\genfrac{}{}{0pt}{}{L}{R}$ and we do not need to specify which set of factors goes with which Feynman diagram.

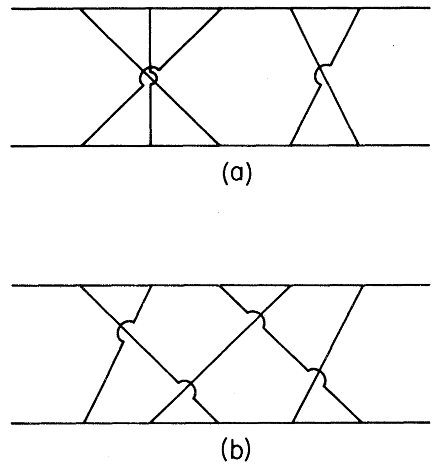

FIG. 18. Two contributing tenth-order Feynman diagrams.

We construct the sum of all contributing Feynman diagrams by adding vertical lines one at a time to the existing bridge structure. Each line has an isospin matrix that goes with it and at any stage before the end there will be three separate sets of isospin matrices (Fig. 20),

(A) those in the upper line,
(B) those at the left of the lower line, and
(C) those at the right of the lower line.

We denote these 3 sets of isospin matrices by the vector

$$\begin{pmatrix} A \\ B \\ C \end{pmatrix}. \tag{4.1}$$

We denote by $M\binom{i}{j}$ the operation of adding the line $\genfrac{}{}{0pt}{}{i}{j}$ to the existing diagram specified by (4.1).

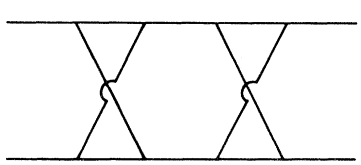

FIG. 17. A contributing eighth-order Feynman diagram.

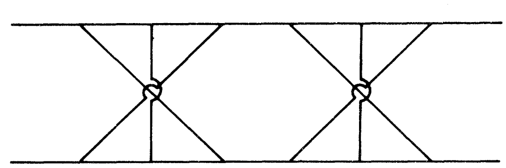

FIG. 19. A contributing twelfth-order Feynman diagram.

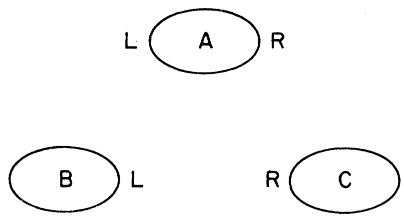

FIG. 20. The 3 sets of isospin matrices discussed in the text.

From (3.7) we find

$$
\begin{aligned}
M\binom{R}{R}\begin{pmatrix}A\\B\\C\end{pmatrix} &= \begin{pmatrix}\sigma_l A\\B\\C\sigma_l\end{pmatrix},\\
M\binom{L}{L}\begin{pmatrix}A\\B\\C\end{pmatrix} &= \begin{pmatrix}A\sigma_l\\\sigma_l B\\C\end{pmatrix},\\
M\binom{R}{L}\begin{pmatrix}A\\B\\C\end{pmatrix} &= -\begin{pmatrix}\sigma_l A\\\sigma_l B\\C\end{pmatrix},\\
M\binom{L}{R}\begin{pmatrix}A\\B\\C\end{pmatrix} &= -\begin{pmatrix}A\sigma_l\\B\\C\sigma_l\end{pmatrix}.
\end{aligned}
\tag{4.2}
$$

Therefore, since we are interested in the sum of all contributing Feynman diagrams we define

$$
M = M\binom{R}{R} + M\binom{L}{R} + M\binom{R}{L} + M\binom{L}{L} \tag{4.3}
$$

and find

$$
M\begin{pmatrix}A\\B\\C\end{pmatrix} = \begin{pmatrix}[\sigma_l, A]\\B\\C\sigma_l\end{pmatrix} - \begin{pmatrix}[\sigma_l, A]\\\sigma_l B\\C\end{pmatrix}. \tag{4.4}
$$

The initial vector which the matrix M operates on is obtained from the sum of the bridge and the crossed bridge of Fig. 21 and is given by

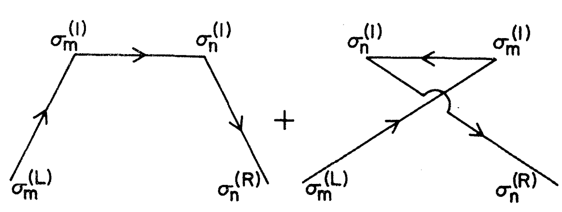

FIG. 21. The two isospin diagrams that give the initial vector.

$$
v_0 = \begin{pmatrix}\sigma_m^{(1)}\sigma_n^{(1)} - \sigma_m^{(1)}\sigma_n^{(1)}\\ \sigma_m^{(L)}\\ \sigma_n^{(R)}\end{pmatrix} = \begin{pmatrix}-\epsilon_{mnl}\sigma_l\\ \sigma_m^{(L)}\\ \sigma_n^{(R)}\end{pmatrix} \tag{4.5}
$$

[where we recall that the commutation relations of the σ_m are given by (1.3a)].

To obtain the sum of all contributing multiple-direct-exchange Feynman diagrams in $(2n+2)$-order perturbation theory we first let the matrix M act on the vector v_0 $n-3$ times. If we call the resulting vector

$$
v_{n-3} = \begin{pmatrix}A^{(n-3)}\\B^{(n-3)}\\C^{(n-3)}\end{pmatrix}, \tag{4.6}
$$

we obtain the sum of all contributing diagrams [up to the factor of $(-1)^{n+1}$ from (3.4)] by using (3.8) to terminate the diagram in either ${}^{RL}_{RL}$, ${}^{LR}_{LR}$, ${}^{RL}_{LR}$, or ${}^{LR}_{RL}$ and then to multiply the factors B and C together (Fig. 22). Therefore this first operation sends

$$
\begin{aligned}
\begin{pmatrix}A\\B\\C\end{pmatrix} &\to \left[\begin{pmatrix}\sigma_n^{(1)}A\sigma_m^{(1)}\\ C\sigma_n^{(2)}\sigma_m^{(2)}B\end{pmatrix} - \begin{pmatrix}\sigma_n(1)A\sigma_m^{(1)}\\ C\sigma_m^{(2)}\sigma_n^{(2)}B\end{pmatrix}\right](-2, 2)\\
&= \begin{pmatrix}\sigma_n^{(1)}A\sigma_m^{(1)}\\ -C\epsilon_{nml}\sigma_l^{(2)}B\end{pmatrix}(-2, 2),
\end{aligned}
\tag{4.7}
$$

where in the two-component vectors the matrices in C and B are both labeled by (2) instead of by R and L and the two components of the column are considered to be multiplied together as a direct product.

We may now use (4.4) to compute the effect of the operator M on the two component vector of (4.7) [where we suppress for the moment the

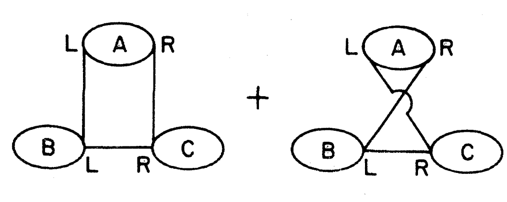

FIG. 22. The two possible ways of terminating the isospin diagrams.

common factor $(-2,2)$]. Thus we find

$$M\begin{pmatrix} \sigma_n^{(1)}A\sigma_m^{(1)} \\ -C\epsilon_{nmk}\sigma_k^{(2)}B \end{pmatrix} = \begin{pmatrix} \sigma_n^{(1)}[\sigma_l^{(1)},A]\sigma_m^{(1)} \\ -\epsilon_{nmk}C\sigma_k^{(2)}\sigma_l^{(2)}B \end{pmatrix} - \begin{pmatrix} \sigma_n^{(1)}[\sigma_l^{(1)},A]\sigma_m^{(1)} \\ -\epsilon_{nmk}C\sigma_k^{(2)}\sigma_l^{(2)}B \end{pmatrix} = \begin{pmatrix} \sigma_n^{(1)}[\sigma_l^{(1)},A]\sigma_m^{(1)} \\ -\epsilon_{nmk}C(-\epsilon_{lkj}\sigma_j^{(2)})B \end{pmatrix}. \tag{4.8}$$

Because of the initial vector (4.5) we are only interested in cases where A is σ_a. Therefore we compute from (4.8)

$$M\begin{pmatrix} \sigma_n^{(1)}\sigma_a^{(1)}\sigma_m^{(1)} \\ -C\epsilon_{nmk}\sigma_k^{(2)}B \end{pmatrix} = \begin{pmatrix} \sigma_n^{(1)}\epsilon_{lab}\sigma_b^{(1)}\sigma_m^{(1)} \\ -\epsilon_{nmk}\epsilon_{lkj}C\sigma_j^{(2)}B \end{pmatrix}. \tag{4.9}$$

Now

$$\epsilon_{lab}\epsilon_{lkj} = \delta_{ak}\delta_{bj} - \delta_{aj}\delta_{bk} \tag{4.10}$$

and hence

$$M\begin{pmatrix} \sigma_n^{(1)}\sigma_a^{(1)}\sigma_m^{(1)} \\ -C\epsilon_{nmk}\sigma_k^{(2)}B \end{pmatrix} = \begin{pmatrix} \sigma_n^{(1)}\sigma_b^{(1)}\sigma_m^{(1)} \\ -\epsilon_{mna}C\sigma_b^{(2)}B \end{pmatrix} - \begin{pmatrix} \sigma_n^{(1)}\sigma_b^{(1)}\sigma_m^{(1)} \\ -\epsilon_{mnb}C\sigma_a^{(2)}B \end{pmatrix}. \tag{4.11}$$

To proceed further we must show that $\epsilon_{mna}\sigma_n\sigma_b\sigma_m$ is symmetric in a and b. To do this we first write

$$\begin{aligned}\epsilon_{mna}\sigma_n\sigma_b\sigma_m &= \tfrac{1}{2}\epsilon_{mna}\{\sigma_n\sigma_b\sigma_m - \sigma_m\sigma_b\sigma_n\} \\ &= \tfrac{1}{2}\epsilon_{mna}(\sigma_n\sigma_b\sigma_m - \sigma_n\sigma_m\sigma_b + \sigma_n\sigma_m\sigma_b \\ &\quad - \sigma_m\sigma_n\sigma_b + \sigma_m\sigma_n\sigma_b - \sigma_m\sigma_b\sigma_n)\end{aligned} \tag{4.12}$$

and then use the commutation relation (1.5a) to obtain

$$\epsilon_{mna}\sigma_n\sigma_b\sigma_m = \tfrac{1}{2}\epsilon_{mna}(-\sigma_n\epsilon_{bml}\sigma_l - \epsilon_{nml}\sigma_l\sigma_b - \sigma_m\epsilon_{nbl}\sigma_l). \tag{4.13}$$

Then we use (4.10) and find

$$\begin{aligned}\epsilon_{mna}\sigma_n\sigma_b\sigma_m &= \tfrac{1}{2}[\sigma_n\sigma_l(\delta_{nb}\delta_{al} - \delta_{nl}\delta_{ab}) \\ &\quad + \sigma_l\sigma_b(\delta_{nn}\delta_{al} - \delta_{nl}\delta_{an}) \\ &\quad + \sigma_m\sigma_l(\delta_{mb}\delta_{al} - \delta_{ml}\delta_{ab})] \\ &= \sigma_a\sigma_b + \sigma_b\sigma_a - \delta_{ab}\vec{\sigma}^2,\end{aligned} \tag{4.14}$$

which is clearly symmetric in a and b.

We now use (4.14) to rewrite the first term on the right-hand side of (4.11) and find

$$M\begin{pmatrix} \sigma_n^{(1)}\sigma_a^{(1)}\sigma_m^{(1)} \\ -C\epsilon_{nmk}\sigma_k^{(2)}B \end{pmatrix} = \begin{pmatrix} \sigma_n^{(1)}\sigma_a^{(1)}\sigma_m^{(1)} \\ -C\epsilon_{nmb}\sigma_b^{(2)}B \end{pmatrix} - \begin{pmatrix} \sigma_n^{(1)}\sigma_b^{(1)}\sigma_m^{(1)} \\ -\epsilon_{mnb}C\sigma_a^{(2)}B \end{pmatrix}. \tag{4.15}$$

Moreover, if in (4.14) we set $a=b$ and sum on b we find

$$\epsilon_{mnb}\sigma_n\sigma_b\sigma_m = -\vec{\sigma}^2 \tag{4.16}$$

and hence the second term in (4.15) reduces to

$$\begin{pmatrix} \sigma_n^{(1)}\sigma_b^{(1)}\sigma_m^{(1)} \\ -\epsilon_{mnb}C\sigma_a^{(2)}B \end{pmatrix} = \begin{pmatrix} \vec{\sigma}^2 \\ C\sigma_a^{(2)}B \end{pmatrix}. \tag{4.17}$$

Define

$$X = \begin{pmatrix} \sigma_n^{(1)}\sigma_a^{(1)}\sigma_m^{(1)} \\ -C\epsilon_{nmb}\sigma_b^{(2)}B \end{pmatrix} \tag{4.18a}$$

and

$$Y = \begin{pmatrix} \vec{\sigma}^2 \\ C\sigma_a^{(2)}B \end{pmatrix}. \tag{4.18b}$$

Then (4.15) is rewritten as

$$MX = X - Y. \tag{4.19}$$

We next compute MY by first using (4.8) to find

$$\begin{aligned} M^2X &= \begin{pmatrix} \sigma_n^{(1)}[\sigma_l^{(1)},[\sigma_{l'}^{(1)},\sigma_a^{(1)}]]\sigma_m^{(1)} \\ -\epsilon_{nmk}C[\sigma_{l'}^{(2)},[\sigma_l^{(2)},\sigma_k^{(2)}]]B \end{pmatrix} \\ &= \begin{pmatrix} \sigma_n^{(1)}\epsilon_{l'ac}\epsilon_{lcf}\sigma_f^{(1)}\sigma_m^{(1)} \\ -\epsilon_{nmk}\epsilon_{lkd}\sigma_{l'dh}C\sigma_h^{(2)}B \end{pmatrix} \\ &= \begin{pmatrix} \sigma_n^{(1)}\sigma_a^{(1)}\sigma_m^{(1)} \\ -\epsilon_{nmk}C\sigma_k^{(2)}B \end{pmatrix} + \begin{pmatrix} \sigma_n^{(1)}\sigma_k^{(1)}\sigma_m^{(1)} \\ -\epsilon_{nmk}C\sigma_a^{(2)}B \end{pmatrix} \\ &= X + Y \end{aligned} \tag{4.20}$$

and hence

$$MY = -2Y. \tag{4.21}$$

Thus in the space spanned by the vector $\binom{X}{Y}$ we may write M as the 2×2 matrix

$$M = \begin{pmatrix} 1 & -1 \\ 0 & -2 \end{pmatrix}. \tag{4.22}$$

Then it is a simple matter to find

$$M^n = \begin{pmatrix} 1 & \frac{1}{3}[-1+(-2)^n] \\ 0 & (-2)^n \end{pmatrix}. \tag{4.23}$$

In terms of this formalism we find that in leading order as $s \to \infty$ the sum of all multiple-direct-exchange Feynman diagrams in $2n+2$ order (for $n \geq 3$) is

$$\mathfrak{M}^{D(n)}_{S(l_1)S(l_2)} \sim -2sg^{2n+2}K_{n+1}(t)(-1)^{n+1}\epsilon_{abc} \times M^{n-3}X^{(0)}_{a;bc}(-2,2), \tag{4.24}$$

where from (4.5) and (4.7) the initial vector $X^{(0)}_{a;bc}$ is

$$X^{(0)}_{a;bc} = \begin{pmatrix} \sigma_n^{(1)}\sigma_a^{(1)}\sigma_m^{(1)} \\ -\epsilon_{nml}\,\sigma_b^{(2)}\sigma_l^{(2)}\sigma_c^{(2)} \end{pmatrix}. \tag{4.25}$$

Therefore with the additional definition of

$$Y^{(0)}_{abc} = \begin{pmatrix} \vec{\sigma}^2 \\ \sigma_b^{(2)}\sigma_a^{(2)}\sigma_c^{(2)} \end{pmatrix}, \tag{4.26}$$

we may use (4.23) to find

$$\epsilon_{abc}M^{n-3}X^{(0)}_{a;bc} = \epsilon_{abc}\{X^{(0)}_{a;bc} + \tfrac{1}{3}[-1+(-2)^{n-3}]\,Y^{(0)}_{abc}\}. \tag{4.27}$$

However, using (4.14)

$$\epsilon_{abc}X^{(0)}_{a;bc} = [\{\sigma_a^{(1)},\sigma_b^{(1)}\} - \delta_{a,b}\vec{\sigma}^2 1^{(1)}] \times [\{\sigma_a^{(2)},\sigma_b^{(2)}\} - \delta_{a,b}\vec{\sigma}^2 1^{(2)}] \tag{4.28}$$

and

$$\epsilon_{abc}Y^{(0)}_{abc} = \vec{\sigma}^{(1)2}\vec{\sigma}^{(2)2}1^{(1)}1^{(2)}, \tag{4.29}$$

where $\{\sigma_a,\sigma_b\} = \sigma_a\sigma_b + \sigma_b\sigma_a$. Finally, define the operator

$$\xi^{(i)}_{a,b} = \{\sigma_a^{(i)},\sigma_b^{(i)}\} - \tfrac{2}{3}\vec{\sigma}^{(i)2}\delta_{a,b}1^{(i)}, \tag{4.30}$$

which obeys

$$\sum_{a=1}^{3}\xi^{(i)}_{a,a} = 0. \tag{4.31}$$

Then we define the isospin-2 amplitude as

$$2T^{(2)} = \xi^{(1)}_{a,b}\,\xi^{(2)}_{a,b} \tag{4.32a}$$

and the isospin-0 amplitude as

$$T^{(0)} = 1^{(1)}1^{(2)}. \tag{4.32b}$$

Thus

$$\begin{aligned}\epsilon_{abc}X^{0}_{a;bc} &= [\xi^{(1)}_{a,b} - \tfrac{1}{3}\delta_{a,b}\vec{\sigma}^{(1)2}1^{(1)}] \\ &\quad\times[\xi^{(2)}_{a,b} - \tfrac{1}{3}\delta_{a,b}\vec{\sigma}^{(2)2}1^{(2)}] \\ &= 2T^{(2)} + \tfrac{1}{3}\vec{\sigma}^{(1)2}\vec{\sigma}^{(2)2}T^{(0)},\end{aligned} \tag{4.33}$$

and hence, using (2.2a), (4.27), (4.29), (4.32), and (4.33) in (4.24), we obtain the final result (1.1).

ACKNOWLEDGMENT

We thank Professor Chen Ning Yang for the most helpful discussions. Professor Yang has also generalized most of the considerations of this paper from SU_2 to an arbitrary semisimple Lie group.

*Work supported in part by the U. S. Atomic Energy Commision Contract No. AT(11-1)-3227.

†Work supported in part by the National Science Foundation under Grant No. DMR73-07565 A01.

[1]B. M. McCoy and T. T. Wu, Phys. Rev. Lett. 35, 604 (1975); Phys. Rev. D 12, 3257 (1975); 13, 1076 (1976); C. Y. Lo and H. Cheng, *ibid.* 13, 1131 (1976); H. T. Nieh and Y. T. Yao, *ibid.* 13, 1082 (1976); C. Tyburski, *ibid.* 13, 1107 (1976); V. S. Fadin, E. A. Kuraev, and L. N. Lipatov, Phys. Lett. 60B, 50 (1975).

[2]B. M. McCoy and T. T. Wu, Phys. Rev. D 13, 369 (1976); 13, 379 (1976); 13, 395 (1976); 13, 424 (1976); 13, 484 (1976); 13, 508 (1976) (referred to as papers I–VI); 12, 546 (1975).

[3]H. Cheng and T. T. Wu, Phys. Rev. 182, 1899 (1969).

[4]B. M. McCoy, C. Tracy, and T. T. Wu, unpublished work.

[5]H. Cheng and T. T. Wu, Phys. Rev. 186, 1611 (1969).

[6]H. Cheng and T. T. Wu, Phys. Rev. Lett. 24, 1456 (1970); in *Proceedings of the 1971 International Symposium on Electron and Photon Interaction at High Energies*, edited by N. B. Mistry (Laboratory for Nuclear Studies, Cornell Univ., Ithaca, 1972), p. 147.